Research Article

Effect of piston bowl geometry modification and compression ratio on the performance and emission characteristics of DI diesel engine

S. K. Gugulothu[1]

Received: 7 April 2020 / Accepted: 10 June 2020 / Published online: 18 July 2020

Abstract

The present study describes the experimental investigations carried out to study the influence of modified piston bowl geometry at a constant speed of the combustion, performance and emission characteristics of a direct injection compression ignition diesel engine. The modified piston profiles, namely hemispherical combustion chamber (HCC) and toroidal combustion chamber (TCC), are manufactured with a baseline compression ratio of 17:1, and the effects of compression ratio (16:1, 17:1 and 18:1) are analyzed. Experiments are carried out with pure diesel for low load to full load conditions for better understanding. With an increasing compression ratio of the engine, TCC piston geometry has shown better improvement in brake thermal efficiency, carbon monoxide and hydrocarbon emissions than HCC. However, a slight penalty in NO_x emission is observed with increasing compression ratio and TCC piston geometry. In-cylinder peak pressure, net heat release rate and rate of pressure rise are increased significantly with increasing compression ratio and the use of TCC geometry.

Keywords Toroidal combustion chamber · Hemispherical combustion chamber · Exhaust gas recirculation · Compression ratio · Performance and emission characteristics

Abbreviations

deg CA	Degree crank angle
DI	Direct injection
HRR	Heat release rate (J/deg CA)
ASTM	American Society for Testing Materials
HCC	Hemispherical combustion chamber
TCC	Toroidal combustion chamber
CO	Carbon monoxide
NO_x	Oxides of nitrogen
HC	Hydrocarbon
EGR	Exhaust gas recirculation
CI	Compression ignition
BTE	Brake thermal efficiency
EGT	Exhaust gas temperature
CC	Combustion chamber
NA	Naturally aspirated
A–F	Air–fuel ratio

1 Introduction

The annual energy outlook revealed that the total energy consumption for transportation sector was 38% and global liquid fuel consumption was 68% in the year 2018 and if it continues in the same way, then the usage of the liquid fuel for transportation sector may rise up to 72% in 2035 [1]. In Indian transportation sector, compression ignition (CI) engines are contributing a major share because of which the original engine manufacturers (OEMs) are striving to achieve high performance and low emissions to meet Bharat stage VI emission norms that are to be implemented w.e.f. April 1, 2020. Homogeneous charge compression ignition (HCCI) technology is a promising one that targets both performance and emissions of CI engines. The HCCI combustion process has the potential to reduce NO_x and particulate emissions, while achieving high thermal

S. K. Gugulothu, santoshgk1988@gmail.com | [1]Department of Mechanical Engineering, National Institute of Technology, Tadepalligudem, Andhra Pradesh, India.

efficiency [2–4]. However, it has a major drawback, higher HC and CO emissions and uncontrolled combustion when fueled with high cetane rating fuel like diesel [5]. Little modification on naturally aspirated CI engine may make it possible to commercialize HCCI technology. In this context, design of combustion chamber (CC) plays a vital role in achieving better performance and emissions characteristics of direct injection CI engines. At the other hand, performance, combustion and emission characteristics of CI engines can be better only when high degree of air swirl and turbulence takes place in the combustion chamber during suction and compression strokes. The swirl–squish interaction in the combustion chamber produces the turbulent flow field when the piston moves toward TDC which could be obtained by changing the default piston geometry of hemispherical combustion chamber (HCC) [6–8]. In order to meet the mandated emission norms, it is important to provide alteration in the piston bowl geometry for better air–fuel mixing throughout the combustion chamber thereby reducing emissions as well as elevated engine performance [9, 10]. With the use of smaller piston bowl size, it is possible to obtain the better swirl and high heat release rate (HRR) [11]. However, by increasing piston bowl radius, engine characteristics may affect adversely. Brijesh et al. investigated numerically and achieved the high turbulence intensity in various combustion chambers such as double lip, Mexican hat, bow and toroidal [12]. It was found that toroidal combustion chamber created better turbulence out of all the combustion chambers [12]. Jaichandar et al. [13] investigated the effect of toroidal re-entrant combustion chamber (TRCC) and hemispherical combustion chamber (HCC) on brake thermal efficiency (BTE) and emission characteristics of a single cylinder direct injection CI engine. It was found that the BTE was 33.07% with TRCC and 31.48% with HCC. Huge reduction of 20.7% in hydrocarbon (HC) emissions was also noted with TRCC. NO_x was increased by 9% in TRCC, i.e., 784 ppm and 712 ppm for TRCC and HCC, respectively. Jyothi et al. had investigated the effect of TCC geometry on a single cylinder CI engine [14]. It was found that BTE increased by 2.94%, and BSFC decreased by 1.3% as compared to HCC geometry. HC and CO emissions were decreased by 2 and 3.5%, respectively. However, NO_x emissions increased by 3.5% by using TCC geometry [14]. The detailed literature as shown in Table 1 ascertained that TCC geometry had shown better engine characteristics over HCC geometry except increased NO_x emissions.

Many researchers have obtained improved results on engine performance mainly brake thermal efficiency and emission characteristics such as HC and CO from CI engines when TCC has been used [13, 14, 28]. However, the marginal increment was found in NO_x emissions due to high temperature rise during combustion. To control the increased NO_x emissions in CI engine, two best possible ways can be adopted, either the use of exhaust gas recirculation (EGR) [29, 30] or reduction in compression ratio [31]. By using the above two solutions to control NO_x emissions, the uncontrolled combustion limitation of HCCI can also be resolved. The main motive of the current investigation was to enhance performance and reduce emissions of a conventional CI engine by incorporating two methodologies, i.e., compression ratio increment

Table 1 Comparison of piston bowl geometry effect on single cylinder

Piston bowl	Engine specifications	Results compared with HCC							Ref.
		BTE	BSFC	CO	HC	NO_x	P	HRR	
TCC and TPCC	1500 rpm, CR 18:1, IP 210 bar	↑	↓	↓	↓	↑	↑	↑	[15]
TCC and TRCC	1500 rpm, CR 17.5:1, IP 210 bar	↑	↓			↑			[16]
TPCC and TCC	1500 rpm, CR 17.5:1	↑	↓	↓	↓	↑	↑	↑	[17]
TCC and TRCC	CR 17.5:1, RP 3.5 kW, IP 220 bar	↑		↓		↑		↑	[18]
TCC	RP 5.2 kW, IP 220 bar, CR 19.5:1	↑		↓	↓	↑	↑	↑	[19]
TCC and TRCC	1500 rpm CR 18:1, RP 5.2 kW, IP 210 bar	↑	↓	↓	↓	↑	↑	↑	[20]
TCC and HSCC	1700 rpm, CR 18:1, RP 4.5 kW, IP 185 bar,	↑	↓	↓	↓	↑			[21]
TCC, HCC and SCC	1500 rpm, CR 17.5:1, RP 3.5 kW	↑	↓	↓	↓	↑	↑	↑	[22]
HCC, CB1, CB2 and TCC	1500 rpm, CR 17.5:1, RP 3.5 kW	↑	↓	↓	↓	↑	↑	↑	[23]
HCC, SCC and TCC	1500 rpm, CR 17.5:1, RP 3.5 kW	↑	↓	↓	↓	↑	↑	↑	[24]
CB1, CB2, CB3 and CB4	1500 rpm, CR 17.5:1, RP 5.2 kW	↑	↓	↓	↓	↑	↑	↑	[25]
6-Wave and standard w-bowl	1500 rpm, CR 17.5:1, RP 3.5 kW	↑	↓	↓	↓	↑	↑	↑	[26]
MSB, DSB and BB	8000 rpm, CR 17.5:1, RP 5.3 kW	↑	↓	↓	↓	↑	↑	↑	[27]

Four-stroke, DI, CI engine characteristics

TPCC trapezoidal combustion chamber, *TCC* toroidal combustion chamber, *HCC* hemispherical combustion chamber, *HSCC* hemisphere combustion chamber, *RP* rated power, *IP* injection pressure, *P* in-cylinder pressure and piston modification to TCC geometry. Jaichandar and Annamalai investigated the combined effect of high injection pressure and toroidal combustion chamber (TCC) on CI engine and found that engine performance and emissions were improved with TCC and high injection pressure combination. However, an increase in injection pressure was found responsible for NO_x emissions increment due to increased HRR and peak in-cylinder pressure during combustion [32]. Therefore, in the current research one of the key engine design parameters, combustion chamber modification was done. Sagaya Raj et al. [33] studied the air motion for four different geometries for a single cylinder CI engine. They reasoned out that combustion bowl profile played a key role in air–fuel mixing. Performance, combustion and emission characteristics of a diesel engine depend on operating parameters and fuel properties [34] because this diesel engine has to achieve better air movement squish, swirl and turbulence.

This work would also make the existing engine ready to implement HCCI retrofit in order to attain BS-VI emission norms. Experiments were conducted to investigate the combined effect of compression ratio and piston geometry on a single cylinder direct injection CI engine with two different combustion chambers HCC (default geometry) and TCC (modified). The engine was run with three compression ratios (CRs) 16:1, 17:1 and 18:1 and 10% exhaust gas recirculation (EGR).

2 Experimental methodology

Variable compression ratio (VCR), single cylinder, water-cooled engine experimental test setup is shown in Fig. 1. Remaining details of the engine setup are shown in Table 2. Engine setup is equipped with rotameter to control water flow rate, which circulates around the engine and around calorimeter at the range of [illegible]0 L (liter) and 250 L per hour, respectively. The engine was made to operate on VCR, in which engine block was tilted to suitable scale and desired values of compression ratio that was obtained without stopping the engine.

Table 2 Technical specifications of the test engine

Make	Kirloskar TV1
Engine power	3.7 kW
Engine speed	1500 rpm
Cylinder bore and stroke	87.5 mm and 110 mm
Compression ratio range	12:1 to 18:1
Cubic capacity	661 cc
Piston bowl shape	Hemispherical
Piston bowl diameter	52 mm
In-center piston bowl depth	25 mm
Material and thickness of piston	Cast aluminum, thickness 5 mm
Fuel injector pressure range	243 bar @ full load
Fuel injection timing	23 °b TDC

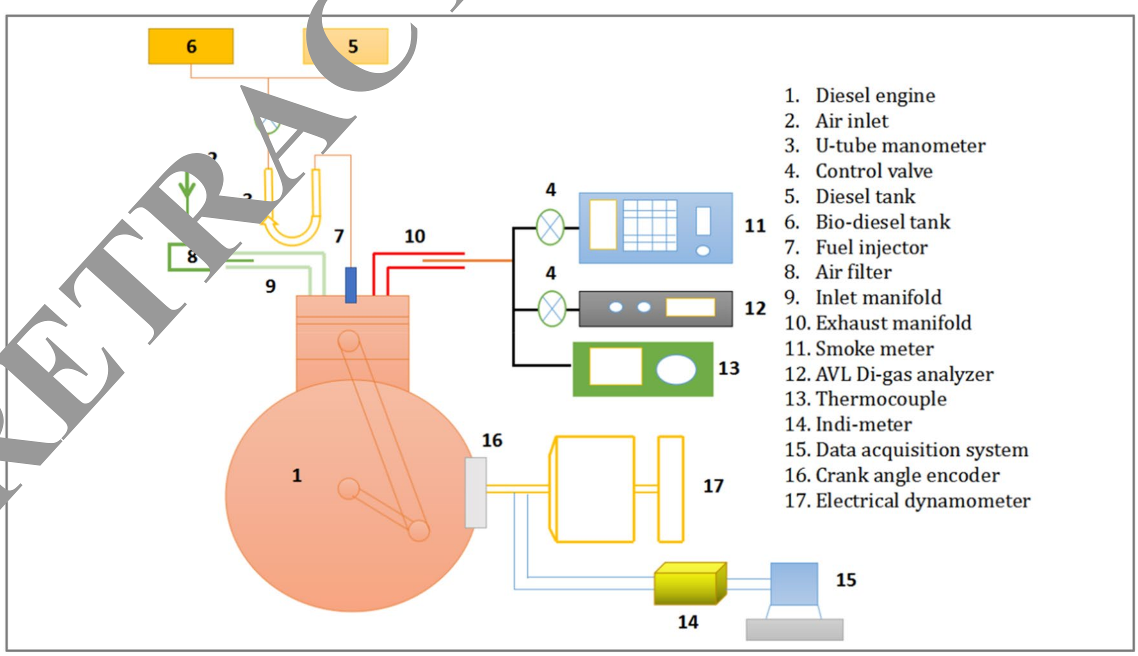

Fig. 1 Schematic diagram of variable compression engine experimental setup using EGR

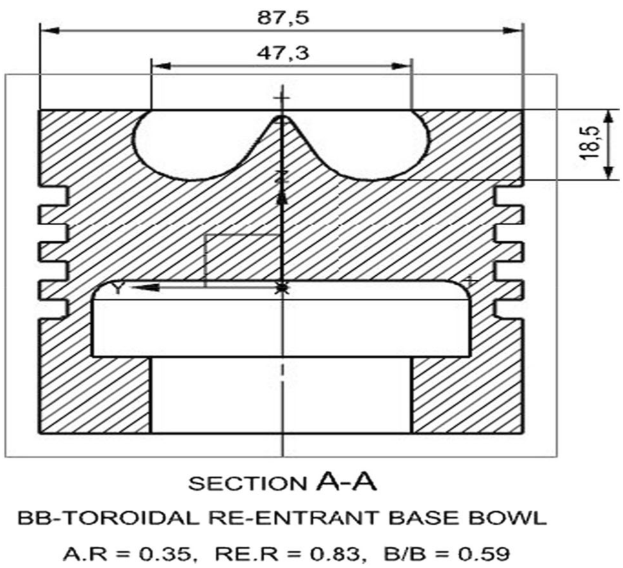

Fig. 2 Toroidal combustion chamber

2.1 Compression ratio adjustment

Conventionally available engine with fixed CR was modified to variable compression ratio (VCR) by providing extra variable combustion space. Tilting cylinder block method was used to vary the CR without changing the piston bowl geometry. With this method, the compression ratio can be changed within range from 12:1 to 18:1 CR without stopping the engine at no load condition. The CR was varied by changing the clearance volume and by keeping the constant swept volume of the engine. The arrangement of the variable compression ratio setup is depicted in Fig. 1. One of the important goals of this research was to reduce the HC and CO emissions of the engine with low NO_x emissions. Therefore, experiment was done on three compression ratios ranging from 16:1 to 18:1. With the earlier experimental results, it was observed that the engine-out HC emissions were increased drastically at below 16:1 CR due to poor combustion characteristics; hence, the present study was investigated for the CR beyond 16:1.

2.2 Modification in combustion chamber of standard engine

The in-cylinder air motion, fuel injection timing, injection pressure and bowl dimensions are some of the important parameters that govern the performance, combustion and emission characteristics of engines [35]. To attain the improved performance and low emissions from the CI engine, quality of A–F mixture is the most important controlling parameter. Quality of air–fuel mixing can be achieved either by increasing injection pressure or compression ratio. In this research, to optimize the performance, combustion and emissions characteristic of an engine the hemispherical combustion chamber (HCC) geometry (Fig. 2) was replaced with a toroidal combustion chamber (TCC) (Fig. 2). Volumes of both the piton cavities were kept same. default (HCC) piston cavity volume provided by OEM was [illegible] cubic centimeter and for the modified (TCC) was also kept same in order to compare their effect on engine behavior. The simulations were carried out with CATIA V5-R.. to measure the volume and surface area of piston cavity. The surface area obtained with HCC and TCC piston cavity was 508.95 cm^2 and 517.55 cm^2. To ensure the same volume for both the pistons, physical measurements by using an isopropyl alcohol (liquid) were carried out. It can reach easily crevices of the cavity due to its low surface tension property. A flat glass plate with small hole was kept on the piston head. Isopropyl was poured into the piston cavity through burette from the glass hole. Volume was measured from the amount of liquid poured from burette.

Various test results have shown that TCC geometry produces high amounts of NO_x emissions [13, 14, 28] with increasing combustion temperature because of rapid and improved air–fuel mixing. Keeping this factor into consideration, the existing engine setup was operated with exhaust gas recirculation (EGR) to control the NO_x emissions.

Total twelve experiments were performed on the engine to evaluate various output parameters as shown in Table 3.

3 Uncertainty analysis

It is to be observed that in the experimental investigation the possibilities of errors and uncertainties are higher because of the test rig accuracies, regulations and indigenous conditions. In this paper, the square root technique was implemented to the engine trials in order to calculate the uncertainties. The equation is as follows:

$$w_R = \sqrt{\left(\frac{\partial R}{\partial x_1}w_1\right)^2 + \left(\frac{\partial R}{\partial x_2}w_2\right)^2 + \cdots + \left(\frac{\partial R}{\partial x_n}w_n\right)^2}$$

where R is the dependent factor and function of independent variables.

The engine parameters like brake power, specific fuel consumption, brake specific energy consumption and brake thermal efficiency are mentioned in "Appendix." The overall uncertainty for the experimental study can be calculated as follows:

Overall uncertainty

$$= \text{Square root of}\left[\begin{array}{l}(\text{uncertainty of MFC})^2+(\text{uncertainty of BTE})^2\\ +(\text{uncertainty of BP})^2+(\text{uncertainty of CO})^2\\ +(\text{uncertainty of HC})^2+\left(\text{uncertainty of NO}_X\right)^2\\ +\left(\text{uncertainty of O}_2\right)^2+\left(\text{uncertainty of CO}_2\right)^2\\ +(\text{uncertainty of EGT})^2\end{array}\right]$$

$$= \text{Square root of}\left[\begin{array}{l}(1.554)^2+(1.764)^2+(0.836)^2+(1.027)^2+(0.839)^2\\ +1.479^2+(0.838)^2+(0.909)^2+(1)^2\end{array}\right]$$

$$= 3.564\%$$

4 Results and discussion

Results obtained from the experiments on the test engine with two different piston geometries HCC and TCC, three different compression ratios 16:1, 17:1 and 18:1 without EGR (Base engine) and 10% EGR are discussed below. Abbreviations used for the discussion are hemispherical combustion chamber without EGR: base-HCC; toroidal combustion chamber without EGR: base-TCC; hemispherical combustion chamber with 10% EGR: EGR–HCC; and toroidal combustion chamber with 10% EGR: EGR–TCC.

4.1 Engine performance improvement

4.1.1 Brake thermal efficiency

Brake thermal efficiency (BTE) was increased with increasing CR for both the piston geometries. However, TCC had shown higher BTE than HCC due to better combustion and rapid evaporation rate of fuel as observed in Fig. 3. At higher compression ratio and full engine load, BTE was decreased by 3% with EGR for both the piston geometries. The decrement in BTE with EGR was observed due to dilution of the A–F mixture. The maximum BTE of 33.12% was achieved with base-TCC, which was higher, by 5.67% than base-HCC. This may be due to better air swirling and turbulence in TCC, which led to better combustion of diesel [12]. Similar trends were observed by Vedhraj et al. with different blends of biodiesel in HCC and TCC engine [18].

4.1.2 Volumetric efficiency

A significant reduction in the amount of intake air to the cylinder was found with addition of EGR as shown in Fig. 4. These deviations were observed because of the change in the intake air temperature. Volumetric efficiency was increased with an increase in compression ratio from 16:1 to 18:1 due to the increase in breathing capacity of the engine. The maximum volumetric efficiency was obtained 91% with base-TCC. There was a marginal enhancement in volumetric efficiency with TCC geometry at all specified conditions than HCC.

4.1.3 Exhaust gas temperature

Variations of exhaust gas temperature (EGT) with change in compression ratios and piston geometries are depicted in Fig. 5. EGT found decreasing with the increase in CR, because of better combustion and reduction in ignition delay as observed in Fig. 8. The use of EGR shows a decrement in EGT due to dilution of A–F mixture. Heat release rate during combustion decreases with EGR addition and causes the EGT reduction. At full engine load, EGT was decreased by almost 9% at 18:1 CR

Table 3 Properties of pure diesel

Density (kg/m^3)	820
Kinematic viscosity (cSt)	2.9
Calorific value (MJ/kg)	44.12
Flash point (°C)	66
Cetane number	52
Self-ignition temperature (°C)	300
Latent heat of evaporation (kJ/kg)	300
Molecular weight	170
Solubility	Immiscible

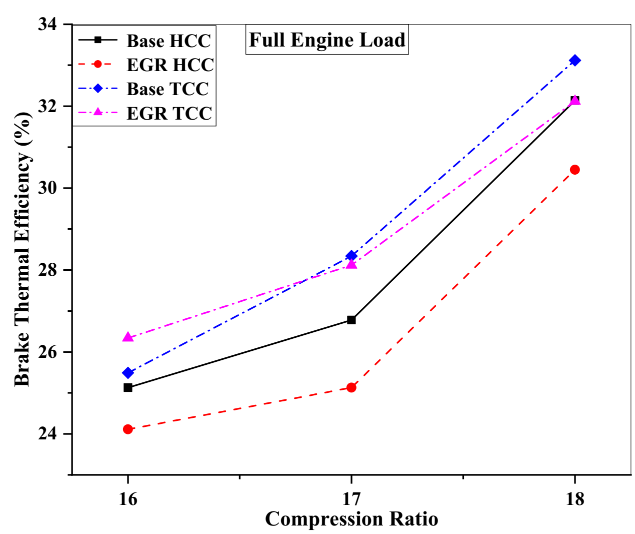

Fig. 3 Brake thermal efficiency at full engine load at various compression ratios without EGR and 10% EGR

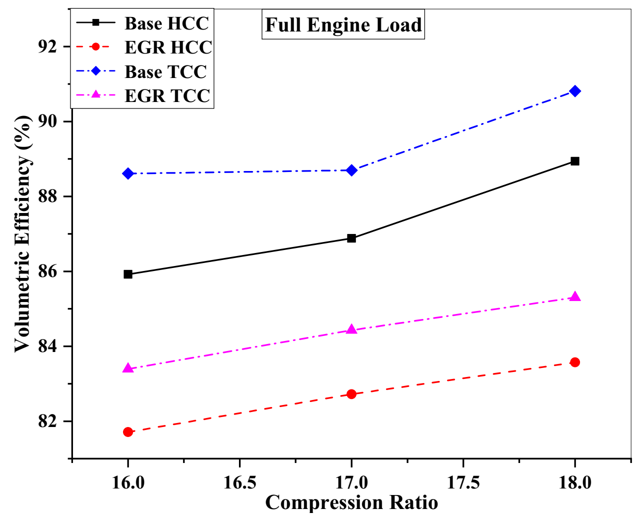

Fig. 4 Volumetric efficiency at full engine load at various compression ratios without EGR and 10% EGR

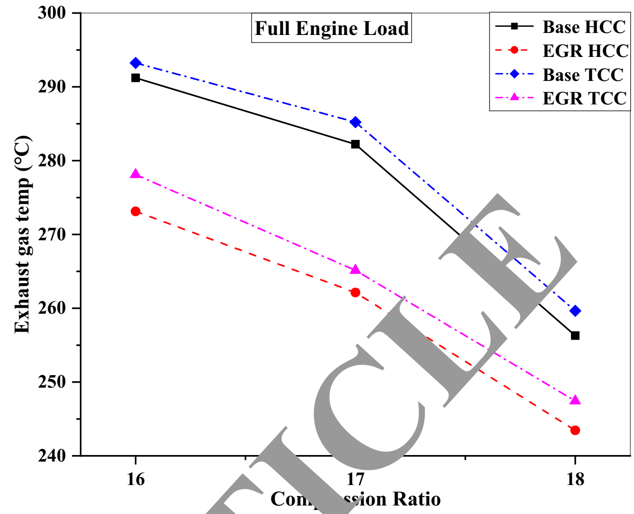

Fig. 5 Exhaust gas temperature at full engine load at various compression ratios without EGR and 10% EGR

when compared between base-HCC and EGR–HCC. The maximum EGT was achieved about 292 °C with base-TCC, and rapid combustion led to the shorter duration in burning the A–F mixture which in turn increases the overall combustion temperature. The same trend of decreasing EGT with the increase in CR had obtained by Hariram and Vagesh [36].

4.2 Engine combustion characteristics

4.2.1 In-cylinder pressure and net heat release rate

Cylinder pressure for full engine load at compression ratios 16:1 to 18:1 with and without EGR was plotted and analyzed as shown in Fig. 6. The peak in combustion pressure occurred slightly near TDC as the compression ratio increased from 16:1 to 18:1 for both the HCC and TCC geometries. At the same engine load, the peak pressure for base-TCC (60.[illegible] bar) at 18:1 CR is higher than HCC (56.31 bar) by 7.45% as shown in Fig. 6b.

The use of EGR showed the negative effect on combustion characteristics of an engine. It is because of increment in the intake charge specific heat capacity and reduction in O_2 availability. EGR led to decrease in the in-cylinder pressure during combustion and so combustion temperature and is depicted in Fig. 7. At full engine load, the maximum heat release was observed with base-TCC (47.06 J/° CA) at 18:1 CR and also found that peak point of heat release rate was approaching near TDC with an increase in CR. The negative heat release was observed at all engine loads because of the heat transfer to the cylinder surfaces.

4.2.2 Ignition delay

Ignition delay of fuel is an important parameter in determining the knocking behavior of CI engines. Figure 8 shows the variation of ignition delay for various compression ratios and 10% EGR at full engine load. It has been observed that the ignition delay periods for TCC are lower than HCC at all specified engine operating conditions. Due to rapid mixing of A–F mixture in TCC, fuel attains the self-ignition temperature in short span of time, and hence, delay period decreases in such a combustion chamber [13]. Ignition delay period was increased with EGR with HCC and TCC, and it is noticed from Table 4. Ignition delay period (crank angle) for all the operating conditions is converted to time (ms) by Eq. 1. At 18:1 CR, ignition delay was decreased by almost 24% with base-TCC than base-HCC:

$$T(\mathrm{ms}) = \left[\frac{\text{delay period (CA)}}{((\mathrm{rpm}/60) * 360)} * 1000 \right] \tag{1}$$

4.2.3 Rate of pressure rise

Rate of pressure rise (ROPR) indicates combustion roughness, and it is a crucial parameter in the entire engine operation. The higher the ROPR means the maximum amount of injected fuel is burnt during the pre-mixed combustion phase [37].

Figure 9 shows the comparison of ROPR at various compression ratios and 10% EGR at full engine load. The maximum peak in ROPR was found to be 3.47 bar/°CA 2° bTDC with base-TCC, whereas for base-HCC, it was 3.36 bar/°CA 3°

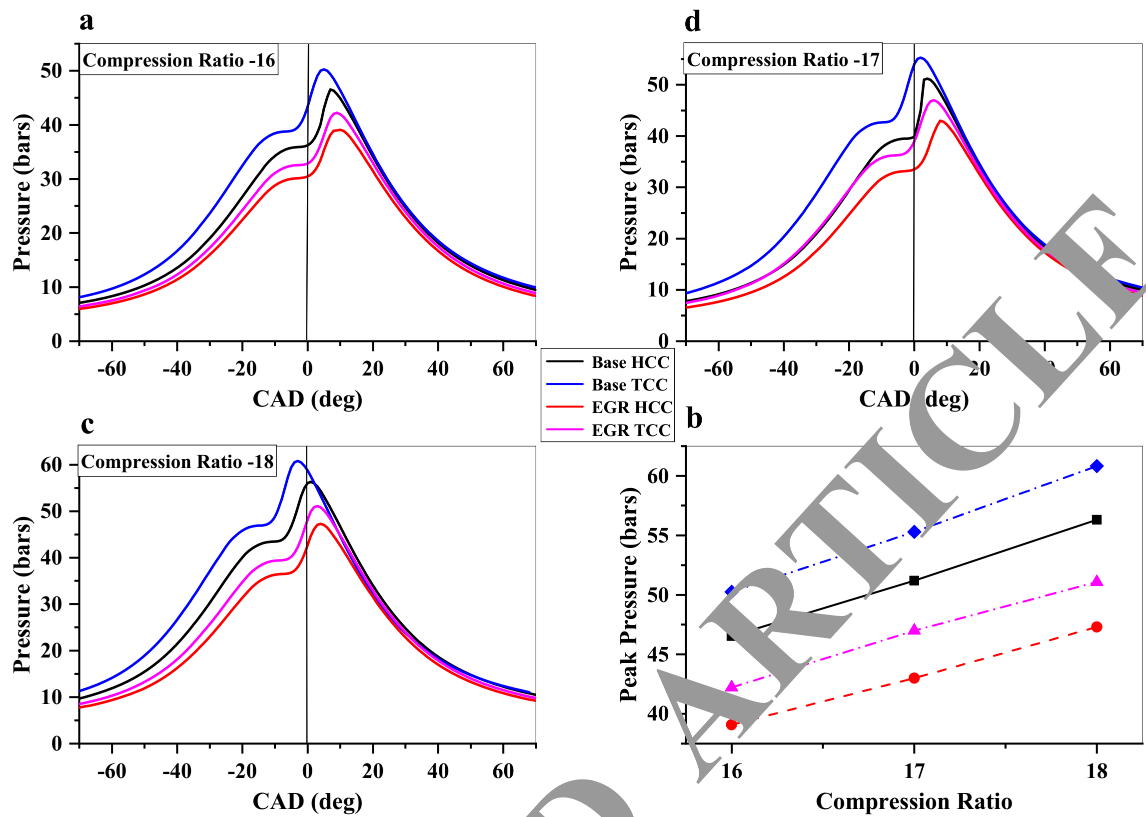

Fig. 6 In-cylinder pressure at various compression ratios and 10% EGR at full engine load

aTDC at 18:1 CR which is lower than base-TCC with a small margin. It shows that combustion phenomena in both the piston geometries is almost the same. On the other side, the minimum peak in ROPR was 1.77 bar/°CA occurred at 16:1 CR with EGR–HCC. The density of A–F mixing decreases as the compression ratio reduced and further decreased with EGR which decreases the HRR during combustion.

4.3 Engine emissions reduction

4.3.1 NO_x emissions

NO_x emissions are produced at high combustion temperature, and it depends on several engine parameters like compression ratio, piston bowl geometry, equivalence ratio, etc.[38]. It is noticed from Fig. 10 that NO_x emissions were decreased with the use of EGR. This trend was observed due to decrement in O_2 availability because of mixing of partial amount of the O_2 of fresh intake air with recirculated gas [30, 39]. This causes a reduction in the local flame temperature because of the spatial broadening of the flame due to the reduction in the oxygen [40]. In the end, because of endothermic chemical reaction like the dissociation of H_2O and CO_2, the combustion temperature was decreased [41].

At full load and 18:1 CR, NO_x emissions were recorded as 745 ppm for base-TCC, which was maximum among all specified conditions. However, for EGR–TCC it was decreased by 6.4% than base-TCC. EGR–TCC and base-HCC have produced same amount of NO_x emissions at 18:1 CR. It was noticed that NO_x emissions steadily increased with increasing CR. The increment in NO_x emissions was due to reduction in ignition delay and increase in peak pressure, resulting in increasing combustion temperature.

4.3.2 Carbon monoxide emissions

Carbon monoxide (CO) emissions are produced due to incomplete combustion, and it mainly depends on A–F ratio [42]. The use of EGR decreases in-cylinder O_2 availability during combustion and also slows down the reaction rates of the A–F mixture, hence producing lower temperatures [30]. At such a temperature, the flame front propagation could not be sustained with lean mixtures. Thus, the A–F mixture does not combust completely, causing CO emissions as depicted in Fig. 11. It was observed that CO emissions are decreasing with an increase in compression ratio due to better combustion. Being in agreement with references [43, 44], peak in CO emissions was observed as EGR proportion increased in fresh A–F mixture. Minimum

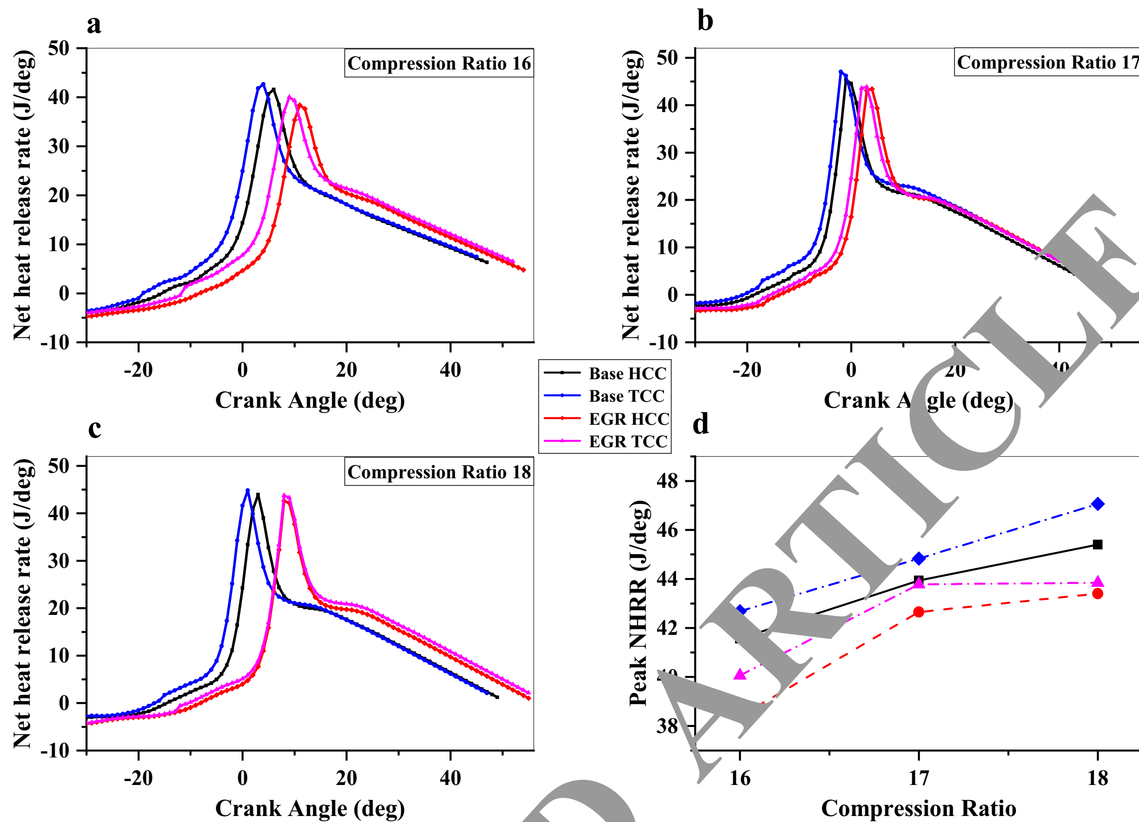

Fig. 7 Net heat release rate at various compression ratios and 10% EGR at full engine load

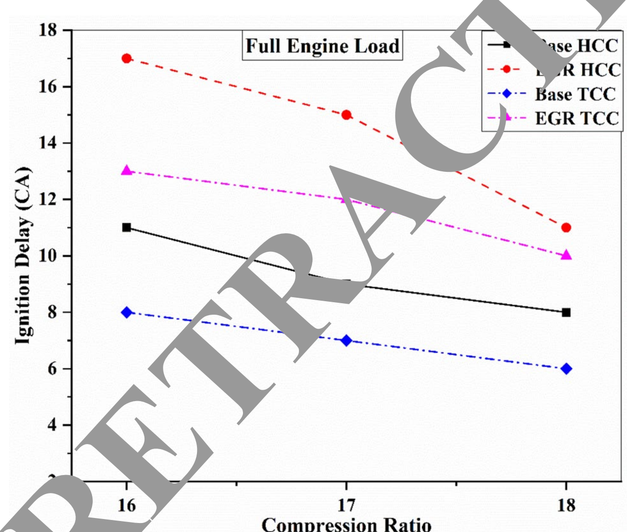

Fig. 8 Ignition delay at various compression ratios and 10% EGR at full engine load

CO emissions (0.05%) were achieved at base-TCC with 18:1 CR. TCC piston geometries had shown lower CO emissions than HCC due to enhanced combustion [13, 17]. An interesting fact came to observation was that the CO emissions for EGR–TCC and base-HCC were almost same at all the compression ratios.

4.3.3 Hydrocarbon emissions

Figure 12 shows the HC emissions at varying compression ratios and 10% EGR at full engine load. It is observed that the HC emissions steadily decrease with increasing compression ratio. This is because the increase in the intake air temperature at the end of compression stroke improves the combustion temperature and reduces the charge dilution that leads to better combustion and reduction in HC emissions. It was seen that with the induction of exhaust gases with fresh charge, HC emissions were increased. Fuel quantity being injected for any specific condition with or without EGR is remained same. Recirculated exhaust gas decreases the O_2 availability for combustion which leads to increase in HC emissions from an engine than the base condition [43]. The maximum value of HC emissions is observed to be 48 ppm at 16:1 CR with EGR–HCC. TCC has shown lower HC emissions at all the specified conditions than HCC; it is due to better mixing of A–F because of improved air swirl [14]. At 18:1 CR, base-TCC has shown

Table 4 Experiments performed on DI engine at full engine load

Piston	Compression ratios	EGR	Output parameters
HCC piston	16:1, 17:1, 18:1	Without EGR 10% EGR	Engine performance Brake specific fuel consumption Brake thermal efficiency Exhaust gas temperature Volumetric efficiency
TCC piston	16:1, 17:1, 18:1	Without EGR 10% EGR	Engine combustion Net heat release rate Pressure rise during combustion Engine emissions Carbon monoxide Hydrocarbon Oxides of nitrogen

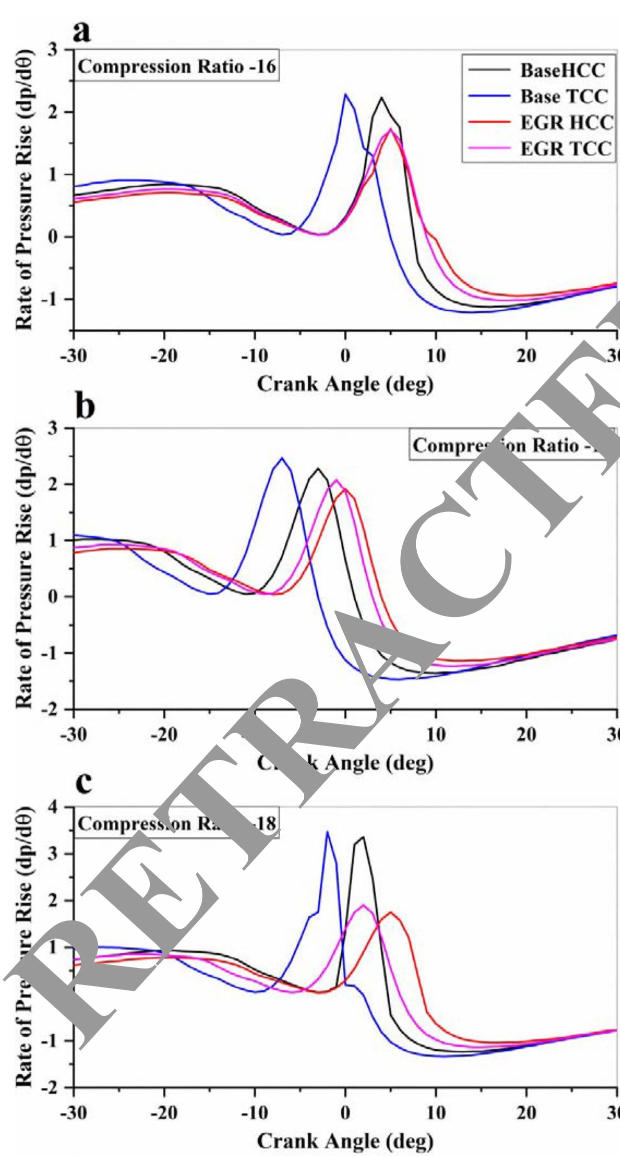

Fig. 9 Rate of pressure rise at various compression ratios and 10% EGR at full engine load

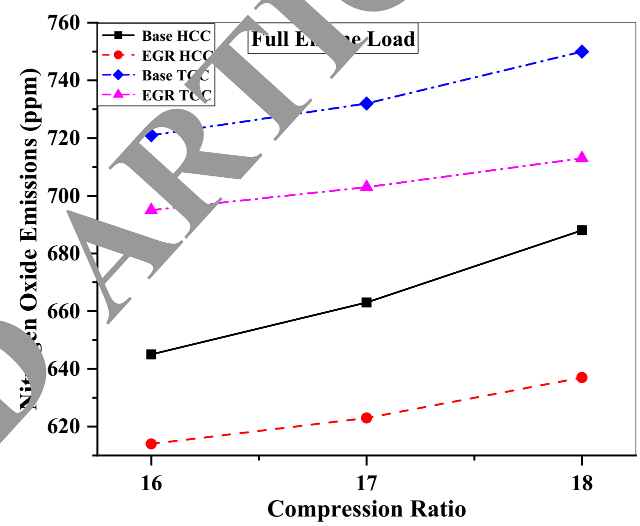

Fig. 10 NO_x at various compression ratios and 10% EGR at full engine load

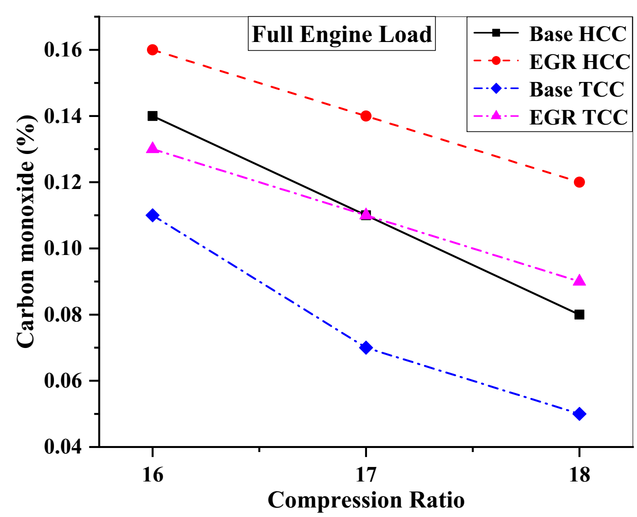

Fig. 11 CO emissions at various compression ratios and 10% EGR at full engine load

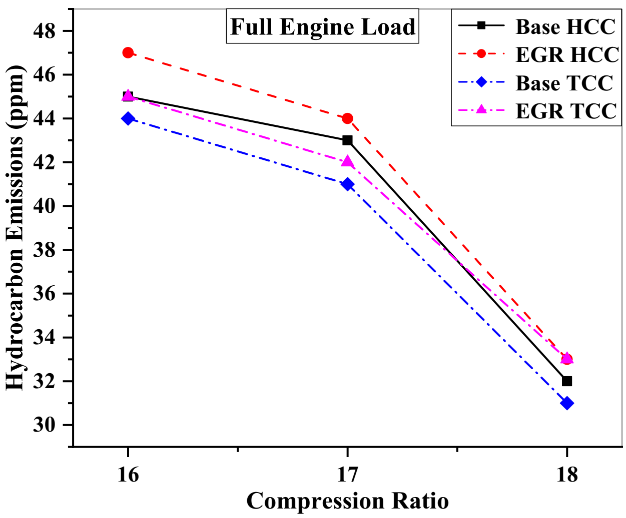

Fig. 12 HC emissions at various compression ratios and 10% EGR at full engine load

8.82% of decrement in HC emissions than base-HCC. Summary of the results is shown in Table 5, which represents the effect of piston geometries, CR and EGR on the engine behavior Table 6.

5 Conclusions

In this research, the effect of toroidal combustion chamber (TCC) geometry on performance, combustion and emissions of a compression ignition (CI) engine with variable compression ratio (CR) and exhaust gas recirculation (EGR) was investigated. The conclusions derived from the present study are encapsulated as below:

- Improved air swirling by the TCC piston enriches the air–fuel mixing and hence enhances the brake thermal efficiency (BTE) than hemispherical combustion chamber (HCC). Maximum BTE achieved with base-TCC was 33.12%, which was higher by 5.67% than base-HCC.
- Transcend combustion as a result of enhanced mixture formation in TCC lowers CO and HC emissions as compared to HCC piston geometry. However, NO_x emissions increased with the increase in compression ratio and decreased with the induction of EGR. NO_x emissions increased with base-TCC by 10.54% than base-HCC, whereas it decreased by 3.19% with EGR–TCC at 18:1 CR. The increment in NO_x emissions was observed due to an increased maximum rate of pressure rise caused by higher air swirl by TCC piston bowl as compared to HCC.

Table 5 Ignition delay period at various compression ratios and 10% EGR in terms of crank angle and time

Compression ratio	Base-HCC		Base-TCC		EGR–HCC		EGR–TCC	
	CA (deg)	Time (ms)	CA (deg)	Time (ms)	CA (deg)	Time (ms)	CA (deg)	Time (ms)
16:1	11	1.22	8	0.88	17	1.88	13	1.44
17:1	9	1.00	7	0.77	15	1.66	12	1.33
18:1	8	0.88	6	0.67	11	1.23	10	1.11

Table 6 Summary of results

Parameter	TCC as compared to HCC	Effect of CR	Effect of EGR
BTE	Increased with use of TCC	Increased with the increase in compression ratio	Decreased with EGR
EGT	Increased with use of TCC	Decreased with an increase in CR	Decreased with EGR
Volumetric efficiency	Higher in TCC	Increased with an increase in compression ratio	Decreased with EGR
In-cylinder combustion pressure	Higher in TCC	Increased with the increase in CR	Decreased with EGR
NHRR	Higher in TCC	Increased with the increase in CR	Decreased with EGR
CO emissions	Lower in TCC	Decreased with an increase in CR	Increased with EGR
HC emissions	Lower in TCC	Decreased with an increase in CR	Increased with EGR
NO_x emissions	Higher in TCC	Increased with an increase in compression ratio	Decreased with EGR

The present study reveals that the performance, emissions and combustion characteristics of variable compression ratio test rig implemented with EGR can be improved by using suitable combustion chamber geometry and compression ratio.

Compliance with ethical standards

Conflict of interest The author declares that they have no competing interests.

Appendix

$$\frac{\Delta N}{N} = \frac{1}{1500} = 0.0667\%$$

$$\frac{\Delta m}{m} = \frac{0.1}{12} = 0.8333\%$$

$$\mathrm{BP} = \frac{2\pi \mathrm{NT}}{60.1000} = \frac{2\pi \mathrm{Nmgl}}{60000} = \frac{2x3.14x1500x12x9.81x0.185}{60000} = 3.421\ \mathrm{kW}$$
$$\frac{\partial \mathrm{BP}}{\partial N} = \frac{2\pi \mathrm{mgl}}{60000} = \frac{2x3.14x12x9.81x0.185}{60000} = 0.00228061$$
$$\frac{\partial \mathrm{BP}}{\partial m} = \frac{2\pi \mathrm{Ngl}}{60000} = \frac{2x3.14x1500x9.81x0.185}{60000} = 0.28507597$$
$$\Delta \mathrm{BP} = \sqrt{\left(\Delta N \frac{\partial \mathrm{BP}}{\partial N}\right)^2 + \left(\Delta m \frac{\partial \mathrm{BP}}{\partial m}\right)^2}$$
$$\Delta \mathrm{BP} = \sqrt{(1x0.00228061)^2 + (0.1x0.28507597)^2}$$
$$\Delta \mathrm{BP} = 0.028598676\ \mathrm{kW}$$
$$\frac{\Delta \mathrm{BP}}{\mathrm{BP}} = \frac{0.028598676}{3.421} = 0.836\%$$

$$\mathrm{MFC} = \frac{fx3600x\rho}{tx1000} = \frac{7.125x3600x0.817}{30x1000} = 0.698535 \frac{\mathrm{kg}}{h}$$
$$\frac{\partial \mathrm{MFC}}{\partial t} = \frac{fx3600x\rho}{(t)^2 x1000} = \frac{7.125x3600x0.817}{30x30x1000} = -0.0232845$$
$$\frac{\partial \mathrm{MFC}}{\partial f} = \frac{3600x\rho}{tx1000} = \frac{3600x0.817}{30x1000} = 0.09804$$
$$\Delta \mathrm{MFC} = \sqrt{\left(\Delta t \frac{\partial \mathrm{MFC}}{\partial t}\right)^2 + \left(\Delta f \frac{\partial \mathrm{MFC}}{\partial f}\right)^2}$$
$$\Delta \mathrm{MFC} = \sqrt{(0.2x - 0.0232845)^2 + (0.1x0.09804)^2}$$
$$\Delta \mathrm{MFC} = 0.010853807 \frac{\mathrm{kg}}{\mathrm{kWh}}$$
$$\frac{\Delta \mathrm{MFC}}{\mathrm{MFC}} = \frac{0.010853807}{0.698535} = 1.554\%$$

$$\mathrm{BSFC} = \frac{\mathrm{MFC}}{\mathrm{BP}} = \frac{0.698535}{3.421} = 0.204190295 \frac{\mathrm{kg}}{\mathrm{kWh}}$$
$$\frac{\partial \mathrm{BSFC}}{\partial \mathrm{BP}} = \frac{\mathrm{MFC}}{(\mathrm{BP})^2} = \frac{0.698535}{(3.421)^2} = -0.059687312$$
$$\frac{\partial \mathrm{BSFC}}{\partial \mathrm{MFC}} = \frac{1}{\mathrm{BP}} = \frac{1}{3.421} = 0.292312219$$
$$\Delta \mathrm{BSFC} = \sqrt{\left(\Delta \mathrm{BP} \frac{\partial \mathrm{BSFC}}{\partial \mathrm{BP}}\right)^2 + \left(\Delta \mathrm{MFC} \frac{\partial \mathrm{BSFC}}{\partial \mathrm{MFC}}\right)^2}$$
$$\Delta \mathrm{BSFC} = \sqrt{(0.028598676x - 0.059687312)^2 + (0.010853807x0.292312219)^2}$$
$$\Delta \mathrm{BSFC} = 0.003602749243 \frac{\mathrm{kg}}{\mathrm{kWh}}$$
$$\frac{\Delta \mathrm{BSFC}}{\mathrm{BSFC}} = \frac{0.003602749243}{0.204190295} = 1.764\%$$

$$= \sqrt{\left(\frac{\Delta \mathrm{CO}}{\mathrm{CO}}\right)^2 + \left(\frac{\Delta \mathrm{BP}}{\mathrm{BP}}\right)^2}$$
$$= \sqrt{(0.00597)^2 + (0.00836)^2}$$
$$= 1.027\%$$

$$= \sqrt{\left(\frac{\Delta \mathrm{CO}_2}{\mathrm{CO}_2}\right)^2 + \left(\frac{\Delta \mathrm{BP}}{\mathrm{BP}}\right)^2}$$
$$= \sqrt{(0.0035587)^2 + (0.00836)^2}$$
$$= 0.909\%$$

References

1. Outlook AE (2002) with projections to 2040. US Energy Information Administration. 2001, DOE/EIA-0383, December
2. Agarwal AK et al (2013) Characterization of exhaust particulates from diesel fueled homogenous charge compression ignition combustion engine. J Aerosol Sci 58:71–85. https://doi.org/10.1016/j.jaerosci.2012.12.005
3. Singh G, Singh AP, Agarwal AK (2014) Experimental investigations of combustion, performance and emission characterization of biodiesel fuelled HCCI engine using external mixture formation technique. Sustain Energy Technol Assess 6:116–128. https://doi.org/10.1016/j.seta.2014.01.002
4. Maurya RK, Agarwal AK (2014) Experimental investigations of performance, combustion and emission characteristics of ethanol and methanol fueled HCCI engine. Fuel Process Technol 126:30–48. https://doi.org/10.1016/j.fuproc.2014.03.031
5. Najt PM, Foster DE (1983) Compression-ignited homogeneous charge combustion, SAE Technical Paper
6. Prasad B et al (2011) High swirl-inducing piston bowls in small diesel engines for emission reduction. Appl Energy 88(7):2355–2367
7. Ogawa H, et al. (1996) Three-dimensional computation of the effects of the swirl ratio in direct-injection diesel engines on NO_x and soot emissions, SAE Technical Paper

8. Arcoumanis C, Bicen A, Whitelaw J (1983) Squish and swirl-squish interaction in motored model engines. J Fluids Eng 105(1):105–112
9. De Risi A, Donateo T, Laforgia D (2003) Optimization of the combustion chamber of direct injection diesel engines, SAE Technical Paper
10. Saito T, et al. (1986) Effects of combustion chamber geometry on diesel combustion, SAE Technical Paper
11. Subramanian S et al. (2016) Piston bowl optimization for single cylinder diesel engine using CFD, SAE Technical Paper
12. Brijesh P, Abhishek S, Sreedhara S (2015) Numerical investigation of effect of bowl profiles on performance and emission characteristics of a diesel engine, SAE Technical Paper
13. Jaichandar S, Annamalai K (2012) Influences of re-entrant combustion chamber geometry on the performance of Pongamia biodiesel in a DI diesel engine. Energy 44(1):633–640
14. Jyothi U, Reddy KV (2017) Experimental study on performance, combustion and emissions of diesel engine with re-entrant combustion chamber of aluminum alloy. Mater Today: Proc 4(2):1332–1339
15. Viswanathan K, Pasupathy B (2017) Studies on piston bowl geometries using single blend ratio of various non-edible oils. Environ Sci Pollut Res Int 24(20):17068–17080. https://doi.org/10.1007/s11356-017-9344-3
16. Khan S, Panua R, Bose PK (2018) Combined effects of piston bowl geometry and spray pattern on mixing, combustion and emissions of a diesel engine: a numerical approach. Fuel 225:203–217. https://doi.org/10.1016/j.fuel.2018.03.139
17. Karthickeyan V (2019) Effect of combustion chamber bowl geometry modification on engine performance, combustion and emission characteristics of biodiesel fuelled diesel engine with its energy and exergy analysis. Energy 176:830–852. https://doi.org/10.1016/j.energy.2019.04.012
18. Vedharaj S et al (2015) Optimization of combustion bowl geometry for the operation of kapok biodiesel–diesel blends in a stationary diesel engine. Fuel 139:561–567
19. Gnanamoorthi V, Marudhan NM, Gobalakichenin D (2016) Effect of combustion chamber geometry on performance, combustion, and emission of direct injection diesel engine with ethanol–diesel blend. Therm Sci 20:937–946
20. Karthickeyan V, Balamurugan P, Ramalingam S (2016) Studies on orange oil methyl ester in diesel engine with hemispherical and toroidal combustion chamber. Thermal Sci 20:981–989
21. Kumar V (2017) Experimental investigation of piston bowl geometry effects on performance and emissions characteristics of diesel engine at variable injection pressure and timings. Int J Ambient Energy 39(7):685–693. https://doi.org/10.1080/01430750.2017.1333041
22. Ganji PR, Singh RN, Raju VRK, Srinivasa Rao S (2018) Design of piston bowl geometry for better combustion in direct-injection compression ignition engine. Sādhanā 43(6):92
23. Dhinesh B, Annamalai M, Lalvani IJ, Annamalai K (2017) Studies on the influence of combustion bowl modification for the operation of Cymbopogon flexuosus biofuel based diesel blends in a DI diesel engine. Appl Therm Eng 112:627–637
24. Kattela SP, Vysyaraju RKR, Surapaneni SR, Ganji PR (2019) Effect of n-butanol/diesel blends and piston bowl geometry on combustion and emission characteristics of CI engine. Environ Sci Pollut Res 26(2):1661–1674
25. Balasubramanian D, Arumugam SRS, Subramani L, Chellakumar IJLJS, Mani A (2018) A numerical study on the effect of various combustion bowl parameters on the performance, combustion, and emission behavior on a single cylinder diesel engine. Environ Sci Pollut Res 25(3):2273–2284
26. Zhang T, Eismark J, Munch K, Denbratt I (2020) Effects of a wave-shaped piston bowl geometry on the performance of heavy duty diesel engines fueled with alcohols and biodiesel blends. Renew Energy 148:512–522
27. Sener R, Yangaz MU, Gul MZ (2020) Effects of injection strategy and combustion chamber modification on a single-cylinder diesel engine. Fuel 266:117122
28. Arumugam S, Pitchandi K, Arventh M, Maheshkumar P (2015) Effect of re-entrant and toroidal combustion chambers in a DICI engine. In: Applied mechanics and materials, vol 787. Trans Tech Publications Ltd, pp 722–726
29. Ladommatos N, Abdelhalim S, Zhao H (2000) The effects of exhaust gas recirculation on diesel combustion and emissions. Int J Engine Res 1(1):107–126
30. Agarwal D, Singh SK, Agarwal AK (2011) Effect of Exhaust Gas Recirculation (EGR) on performance, emissions, deposits and durability of a constant speed compression ignition engine. Appl Energy 88(8):2900–2907
31. Ozawa G (1997) Variable compression ratio engine. Google Patents
32. Jaichandar S, Annamalai K (2013) Combined impact of injection pressure and combustion chamber geometry on the performance of a biodiesel fueled diesel engine. Energy 55:330–339. https://doi.org/10.1016/j.energy.2013.04.019
33. Raj ARGS, Mallikarjuna JM, Ganesan V (2013) Energy efficient piston configuration for effective air motion–a CFD study. Appl Energy 102:347–354
34. Challen B, Baranescu R (1999) Diesel engine reference book. Society of automotive engineers. Bath Press, Bath
35. Ganesan V (2012) Internal combustion engines. McGraw Hill Education (India) Pvt Ltd, Bengaluru
36. Hariram V, Vagesh Shangar R (2015) Influence of compression ratio on combustion and performance characteristics of direct injection compression ignition engine. Alex Eng J 54(4):807–814. https://doi.org/10.1016/j.aej.2015.06.007
37. Selim M, Radwan MS, Elfeky SM (2003) Combustion of jojoba methyl ester in an indirect injection diesel engine. Renew Energy 28(9):1401–1420
38. Heywood JB (1988) Internal combustion engine fundamentals, vol 930. Mcgraw-hill, New York
39. Guo M et al (2015) A short review of treatment methods of marine diesel engine exhaust gases. Proc Eng 121:938–943
40. Hussain J et al (2012) Retracted: effect of exhaust gas recirculation (EGR) on performance and emission characteristics of a three cylinder direct injection compression ignition engine. Elsevier, Amsterdam
41. Maiboom A, Tauzia X, Hétet J-F (2008) Experimental study of various effects of exhaust gas recirculation (EGR) on combustion and emissions of an automotive direct injection diesel engine. Energy 33(1):22–34
42. Park SH, Youn IM, Lee CS (2010) Influence of two-stage injection and exhaust gas recirculation on the emissions reduction in an ethanol-blended diesel-fueled four-cylinder diesel engine. Fuel Process Technol 91(11):1753–1760
43. De Serio D, de Oliveira A, Sodré JR (2017) Effects of EGR rate on performance and emissions of a diesel power generator fueled by B7. J Braz Soc Mech Sci Eng 39(6):1919–1927
44. Kumar BR et al (2016) Effect of a sustainable biofuel–n-octanol–on the combustion, performance and emissions of a DI diesel engine under naturally aspirated and exhaust gas recirculation (EGR) modes. Energy Convers Manag 118:275–286

Publisher's Note Springer Nature remains neutral with regard to jurisdictional claims in published maps and institutional affiliations.